Accepted Manuscript

Submission Date: 2024-04-02
Accepted Date: 2024-04-16
Accepted Manuscript online: 2024-04-17

Synlett

From Protein Structures to Functional Biomimetics

Canan Durukan, Tom N Grossmann.

Affiliations below.

DOI: 10.1055/a-2308-1795

Please cite this article as: Durukan C, Grossmann T N. From Protein Structures to Functional Biomimetics. Synlett 2024. doi: 10.1055/a-2308-1795

Conflict of Interest: T.N.G. is listed as inventors on patent applications related to the INCYPRO stabilization approach as well as β-catenin and RNA-binding peptides. T.N.G. is a co-founder of Incircular B.V. commercializing the INCYPRO technology.

This study was supported by European Research Council (http://dx.doi.org/10.13039/501100000781), 678623, H2020 European Research Council (http://dx.doi.org/10.13039/100010663), 101067731,101112973,839088, Exacte en Natuurwetenschappen (http://dx.doi.org/10.13039/501100024870), 00838037,01291832, Deutsche Forschungsgemeinschaft (http://dx.doi.org/10.13039/501100001659), GR3592/2-1, KWF Kankerbestrijding (http://dx.doi.org/10.13039/501100004622), 15036, Fonds der Chemischen Industrie (http://dx.doi.org/10.13039/100018992), 661413

Abstract:
The development of complex molecular scaffolds with defined folding properties represents a central challenge in chemical research. Proteins are natural scaffolds defined by a hierarchy of structural complexity and have evolved to manifest unique functional characteristics e.g., molecular recognition capabilities that facilitate the binding of target molecules with high affinity and selectivity. Utilizing these features, proteins have been used as a starting point for the design of synthetic foldamers, enhanced biocatalysts as well as bioactive reagents in drug discovery. In this account, we describe the strategies used in our group to stabilize protein folds, ranging from the constraint of bioactive peptide conformations to chemical protein engineering. We discuss the evolution of peptides into peptidomimetics to inhibit protein-protein and protein-nucleic acid interactions, and the selective chemical modification of proteins to enhance their properties for biotechnological applications. The reported peptide- and proteomimetic structures cover a broad range of molecular size and they highlight the importance of structure stabilization for the design of functional biomimetics.

Corresponding Author:
Dr. Tom N Grossmann, VU, Chemistry and Pharmaceutical Sciences, De Boelelaan 1108, 1081 HV Amsterdam, Netherlands, t.n.grossmann@vu.nl

Affiliations:
Canan Durukan, VU, Chemistry and Pharmaceutical Sciences, Amsterdam, Netherlands
Tom N Grossmann, VU, Chemistry and Pharmaceutical Sciences, Amsterdam, Netherlands

From Protein Structures to Functional Biomimetics

Canan Durukan,[a,b] Tom N. Grossmann[a,b,*]

[a] *Department of Chemistry and Pharmaceutical Sciences, Vrije Universiteit Amsterdam, The Netherlands*

[b] *Amsterdam Institute of Molecular and Life Sciences (AIMMS), Vrije Universiteit Amsterdam, The Netherlands*

t.n.grossmann@vu.nl

Keywords: INCYPRO, Peptidomimetic, Protein engineering, Protein-protein interaction, Proteomimetic, Structure-based design

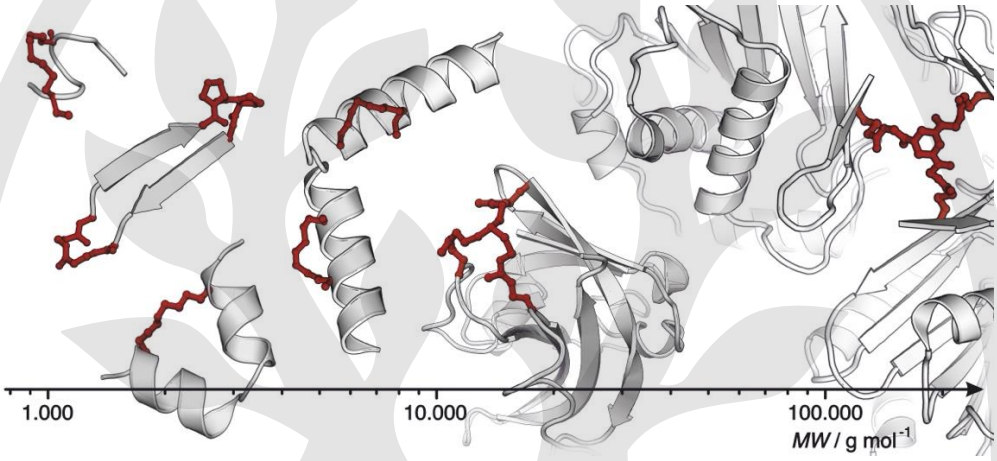

Abstract: The development of complex molecular scaffolds with defined folding properties represents a central challenge in chemical research. Proteins are natural scaffolds defined by a hierarchy of structural complexity and have evolved to manifest unique functional characteristics e.g., molecular recognition capabilities that facilitate the binding of target molecules with high affinity and selectivity. Utilizing these features, proteins have been used as a starting point for the design of synthetic foldamers, enhanced biocatalysts as well as bioactive reagents in drug discovery. In this account, we describe the strategies used in our group to stabilize protein folds, ranging from the constraint of bioactive peptide conformations to chemical protein engineering. We discuss the evolution of peptides into peptidomimetics to inhibit protein-protein and protein-nucleic acid interactions, and the selective chemical modification of proteins to enhance their properties for biotechnological applications. The reported peptide- and proteomimetic structures cover a broad range of molecular size and they highlight the importance of structure stabilization for the design of functional biomimetics.

1 Introduction

2 Constraining the Conformation of Peptides

3 Peptide-Based Covalent Protein Modifiers

4 Chemical Protein Engineering

5 Conclusions

1 Introduction

Proteins have evolved to facilitate diverse cellular functions. For their function, the interplay between the adoption of a defined structure and the possession of intrinsic flexibility is of eminent importance.[1] The unique folding properties of proteins have stimulated a wide range of peptidomimetic and proteomimetic research.[2] Here lately, the interest in peptidomimetic molecules and their use as therapeutic agents became evident.[3] In particular, when aiming for intracellular targets, the installation of sufficient cellular uptake represents a major challenge. To guide the design process and to enable their categorization, we have classified peptidomimetics (Class A – D, Figure 1) based on their resemblance of natural peptides.[3b] This classification not only supports the assessment of the potential and limitations of peptidomimetics in therapeutic settings but also offers a structured approach for their development and optimization.

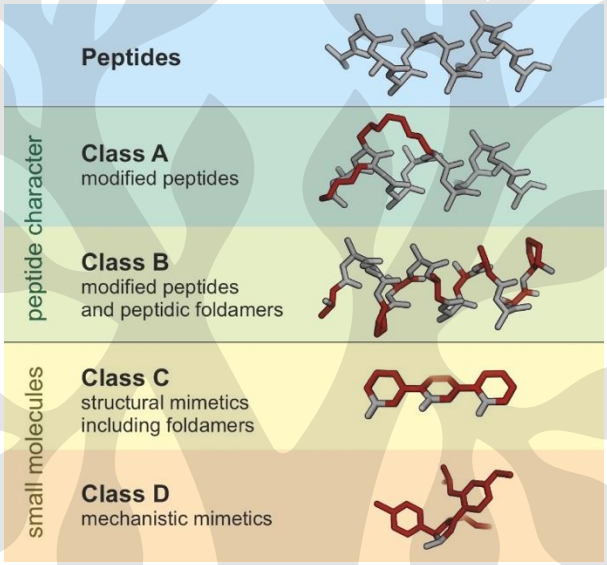

Figure 1| Overview of the peptidomimetic classification with helix mimetics serving as example. Modifications are depicted in red.

Class A mimetics are characterized by moderate modifications, maintaining a high degree of similarity to the original peptide sequence. The primary approach used for obtaining Class A mimetics involves peptide macrocyclization. Further derivatization of Class A peptidomimetics leads to Class B mimetics, which include a larger number of non-natural amino acids and often tend to show higher resistance to proteolytic degradation.[2a] Class A and B mimetics exhibit relatively high similarity to peptides usually rendering their cellular uptake a limiting factor.[4] The defining characteristic of Class C mimetics is their use of small molecular scaffolds to replace the entire peptide backbone. The design process is demanding given the complexity and inherent flexibility of peptide structures. A limited number of Class C mimetics have been studied in a cell-based context, with a focus on α-helix mimetics which tend to lose the selective binding characteristics of their parent peptide sequences.[5] Class D mimetics, identified e.g., through screening methods, offer a unique approach by mimicking the functional mechanism of bioactive peptides without directly imitating their side chain functionalities. However, library composition is an essential factor when aiming for challenging protein targets that lack defined binding pockets.[6]

Our group played an active role in the development of Class A and Class B peptidomimetics using both side chain-to-side chain as well as head-to-tail cyclization approaches. This involved the stabilization of α-helices, β-sheets as well as irregular structural motifs.[7] We have also explored the possibility of stabilizing small tertiary folds for the targeting of proteins which were not addressable with classic peptidomimetic approaches.[8] The idea of introducing chemical crosslinks to stabilize peptide conformations, we have then extended to the stabilization of entire protein domains (tertiary structures)[9] and protein complexes (quaternary structures)[10] resulting in the development of proteomimetic structures with abiotic topologies. In this account, we summarize the efforts of our groups towards the mimicry and stabilization of peptide and protein structures with chemical biology and biotechnological applications.

2 Constraining the Conformation of Peptides

Inhibitors of Protein-Protein Interactions

An early example of a Class A peptidomimetic with a stabilized irregular secondary structure was obtained through the macrocyclization of the 14-3-3 binding epitope of *Pseudomonas aeruginosa*'s virulence factor, exoenzyme S (**ESp**, blue, Figure 2). In collaboration with the group of Christian Ottmann and inspired by hydrocarbon peptide stapling,[11] we have employed ring-closing olefin metathesis (RCM, Figure 2a) to introduce a crosslink which interfaces the target protein 14-3-3 thereby simultaneously constraining the peptide conformation and directly contributing to target interactions.[12] The development of these constrained peptides initially involved the testing of different crosslink lengths and configurations using the 11-mer **ESp** peptide as starting point.[7a] Two architectures were identified, one with an *SS* configuration (referring to the two αC crosslink atoms) using a 12-carbon atom crosslink (**β_{SS}12**, K_d = 41 nM, Figure 2b) and another with an *RS* configuration using an 8-carbon atom crosslink (**β_{RS}8**, K_d = 0.25 μM, Figure 2c). Both mimetics exceed the binding affinity of the linear starting point (**ESp**, K_d = 1.1 μM).

These two scaffolds served as the starting point for subsequent studies. For instance, we showed that the increased affinity of **β_{SS}12** over **β_{RS}8** is likely due to its increased flexibility in the bound state.[13] For **β_{SS}12**, an *in silico* sequence maturation was carried out resulting in Class B peptidomimetic **22** (green, Figure 2b), which involved two non-proteogenic amino acids: *L*-(1-adamantyl)glycine (α) and *L*-γ-carboxyglutamic acid (γ) resulting in a further 2.7-fold increased affinity.[14] Furthermore, our efforts towards peptide miniaturization[15] used **β_{RS}8** as starting point. Here, we noted the importance of the αC-substitution pattern at the crosslinking amino acids. Especially, hydrogen substituents resulted in particularly low affinity (more than 200-fold) relative to the best performing Et/Me pattern in peptidomimetic **11** (yellow, Figure 2c). In addition, we explored alternative crosslinking approaches, such as ring-closing alkyne metathesis (RCAM) instead of RCM also resulting in a mimetic with a high target affinity.[16]

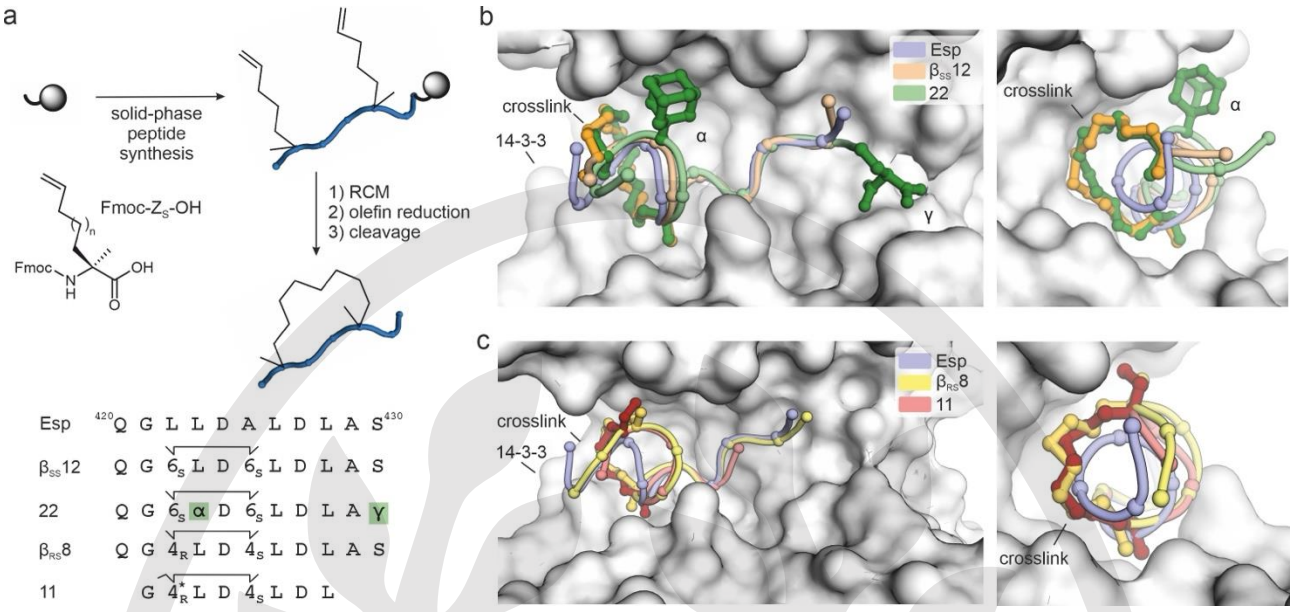

Figure 2 | Inhibitors of 14-3-3-protein interactions. (a) Synthesis of macrocyclic peptides via ring-closing olefin metathesis (RCM) with subsequent double-bond reduction. Fmoc-Z_S-OH is shown as example for an unnatural amino acid (Z = n + 3, number of atoms that contribute to crosslink). (b) Front (left) and side (right) views of overlayed crystal structures of different 14−3−3 (gray surface) bound mimetics derived from **ESp** (blue, PDB ID 4n7g): **β_{SS}12** (wheat, PDB ID 4n84) and **22** (green, PDB ID 5jm4). The crosslinks as well as *L*-(1-adamantyl)glycine (α) and *L*-γ-carboxyglutamic acid (γ) are shown as balls and sticks.[7a,14] (c) Front (left) and side (right) views of overlayed crystal structures of different 14−3−3 (gray surface) bound mimetics derived from **ESp** (blue, PDB ID 4n7g): **β_{RS}8** (yellow, PDB ID 4n7y) and peptide **11** (pink, PDB ID 6rlz).[7a,15] Crosslinks and substituents are shown in balls and sticks.

Hydrocarbon stapled peptides were first reported by Gregory Verdine and colleagues.[11d] They represent Class A helix mimetics in which side-chain-to-side chain crosslinks are installed by RCM. [17] In addition, the crosslinking amino acids feature αC methylation further supporting the helical conformation.[18] In collaboration with the groups of Herbert Waldmann and Roger Goody, we generated hydrocarbon stapled peptides targeting small GTPases from the Rab family.[19] Here, we showed that it is possible to convert Rab-targeting epitopes characterized by very low binding affinities (K_d > 100 µM) into Class A mimetics with one-digit micromolar affinity.[20] Furthermore, improved stability against protease degradation was achieved by including two adjacent hydrocarbon staples.[21] In collaboration with the group of Alois Fürstner, we were able to form one of these staples using RCM and the other one via alkyne metathesis, both occurring in a one-pot reaction.[22]

Stabilized α-helices have also been used to generate peptidomimetic inhibitors derived from the A subunit of the trimeric transcription factor complex NF-Y.[23] Based on a previously reported crystal structure,[24] a 29-mer peptide of NF-YA was used as the initial NF-YB/C-targeting sequence (**PBM**). We performed a truncation study to identify the central 19-mer interaction motif which then served as the starting point for peptidomimetic design. Aiming for stabilization of the central α-helix, hydrocarbon stapling with two different architectures including *i,i*+4 and *i,i*+7 (**2-C**, green) was pursued, however, resulting in only moderately increased binding affinities (Figure 3a). Unexpectedly, when truncating stapled peptide **2-D** N-

terminally, this resulted in a 2.3-fold affinity increase. The substitution of the N-terminal crosslink α-methyl group by hydrogen, providing mimetic **2-D^{N}**, increased binding affinity by a factor of 10. Importantly, this methyl group is not involved in direct contacts with the NF-YB/C target. NMR studies suggest that the initial α-methylation restricts the conformational freedom and forces **2-D** into an all-α-helical confirmation which results in the loss of favorable interactions with NF-YB/C and therefore a loss in binding affinity. Later, we have explored the impact of flexibility in the bound state in more detail.[25] For a truncated version of peptide **2-D^{N}**, crystal structures indicated at least two different accessible conformations when bound to NF-YB/C. This was further supported by molecular dynamics (MD) simulations, overall suggesting that flexibility in the bound state contributes to complex stability.

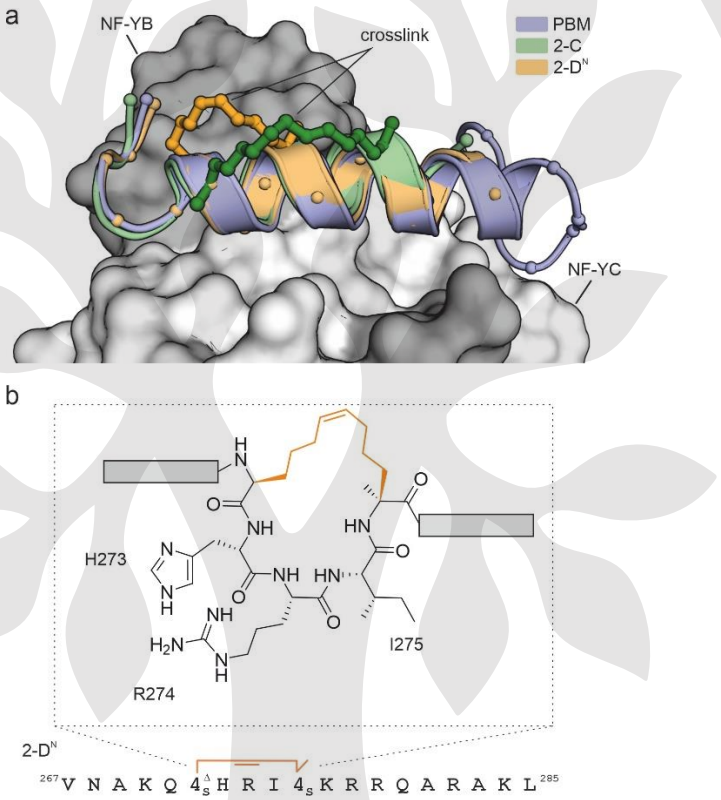

Figure 3| Inhibitors of NF-Y trimer assembly. (a) Superimposition of crystal structures of **PBM** (blue, PDB ID: 6qmp), **2-C** (green, PDB ID: 6qms), and **2-D^{N}** (orange, PDB ID: 6qmq) bound to NF-YB/C (gray surface).[23] (b) Sequence of **2-D^{N}** including chemical structure of central macrocycle.

In collaboration with AstraZeneca and the group of Herbert Waldmann, the helix-turn-helix motif found in the TEAD binding epitope of VGL4[26] (blue, Figure 4a) was stabilized.[8b] Since the individual helices did not provide sufficient affinity, the two-helix arrangement was chosen as the starting point. This motif was stabilized using a lactam bridge between the two helices, resulting in macrocycle **4E** (orange, Figure 4a). To evaluate the activity in cell-based assays, a cell-penetrating peptide was attached, which indeed verified the anticipated modulation of the Hippo pathway. This modulation was confirmed through the analysis of mRNA target gene levels and cell mobility. Another therapeutically relevant protein targeted in our group is the oncogene β-catenin, which serves as a central hub in the Wnt-signalling pathway[27] and showed high

resistance towards targeting with small molecular scaffolds.[28] Our initial β-catenin-targeting efforts focused on the improvement of the cellular uptake of an earlier reported hydrocarbon stapled peptide.[29,30] These sequence maturation efforts resulted in the substitution of arginines by homo-arginine and the addition of a positively charged nuclear localization sequence. Obtained Class B mimetic **NLS-StAx-h** exhibited robust cellular uptake and inhibition of the Wnt-signaling pathway in cell-based assays.[31] Subsequently, we developed a novel β-catenin inhibitor based on a discontinuous anti-parallel β-sheet originating from the protein E-cadherin (blue, Figure 4b).[32] The epitope was first converted into a β-hairpin which was then head-to-tail cyclized providing macrocyclic peptide **12** (orange, Figure 4b).[7b] To enhance cellular uptake, peptide **12** was converted into a bicyclic scaffold by introducing two cysteine residues that were crosslinked using a biselectrophile. To identify a suitable arrangement, different cysteine positions and biselectrophiles were tested providing Class B mimetic **A-b6**, which demonstrated inhibition of Wnt signaling in a Wnt-responsive reporter gene assay (IC_{50} = 8 µM).[7b]

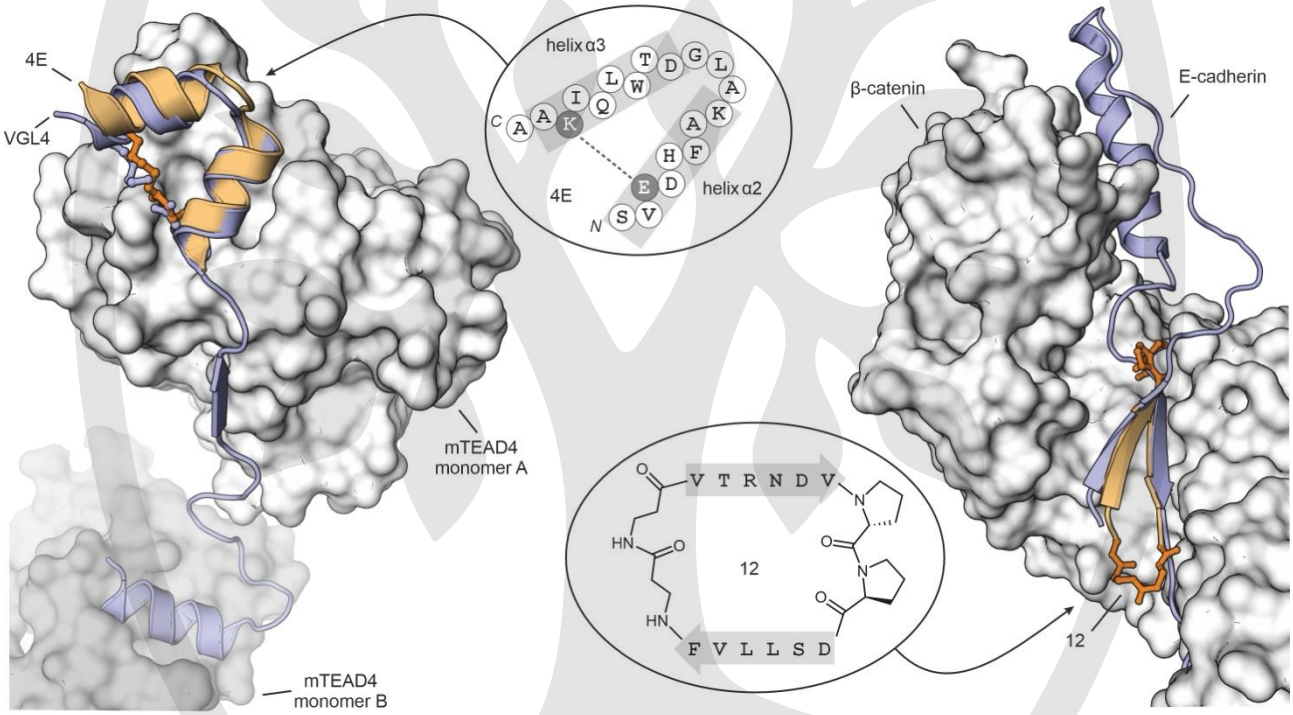

Figure 4| Inhibitors of protein-protein interactions. Left: Overlayed crystal structures of two TEAD monomers (gray surface) bound to VGL4 (blue, PDB ID: 4ln0)[26] and to macrocycle **4E** (orange, PDB ID 6sba).[8b] Right: Overlayed crystal structures of β-catenin (gray surface) bound to a fragment of E-cadherin (blue, PDB ID 1i7x),[32] and to mimetic **12** (orange, PDB ID 7ar4).

RNA-Targeting Peptidomimetics

Peptide-derived molecules have also proven useful to target nucleic acids.[33] Aiming for the design of RNA-binding peptidomimetics, we used the viral protein TAV2b as a starting point. TAV2b binds double-stranded RNA in a sequence-independent manner using two adjacent α-helices that are connected via a short loop (blue, Figure 5a). TAV2b binds siRNA thereby suppressing RNA interference which affects the antiviral

response of plant cells.[34] Guided by a crystal structure of RNA-bound TAV2b, we designed and tested different fragments regarding their RNA binding ability.[35] This resulted in the identification of 33-mer peptide **wt33** binding a palindromic RNA duplex with moderate affinity (K_d = 1.2 µM). In the RNA-bound state, **wt33** contains two helical interaction motifs that, however, were only structured upon binding. To increase their α-helicity, we applied hydrocarbon stapling exploring different architectures. Eventually, double-stapled peptide **B3** with ca. 20-fold increased affinity (K_d = 0.07 µM) and robust cellular uptake was obtained. Interestingly, **B3** also showed an affinity for miRNA-21 (miR21) and its precursor, pre-miR21. Notably, **B3** binding to pre-miR21 resulted in inhibition of miRNA maturation by the nuclease Dicer in a biochemical assay (Figure 5b).[35] Building on these findings, we developed environment-sensitive TAV2b-derived stapled peptides that can serve as a general tool to stabilize double-stranded RNA and support its cellular delivery. Using one of the two TAV2b helices, homo-dimeric, stapled peptide **2'-2'** was designed which contained a disulfide bridge.[36] Dimer binding prolonged the life-time of dsRNA in the medium and also promoted cellular uptake. Importantly, stapled peptide **2'-2'** shows high affinity (K_d = 32 nM) for dsRNA only in its dimeric form, whereas the monomeric stapled peptide exhibits only low affinity (Figure 5c). This gave rise to the ability of the dimer to dissociate from RNA when exposed to reducing conditions, as they can be found in the cytosol. Importantly, our observations indicate that the system acts as a potential carrier for RNA by protecting it in the bloodstream and releasing the RNA cargo in the cytosol.

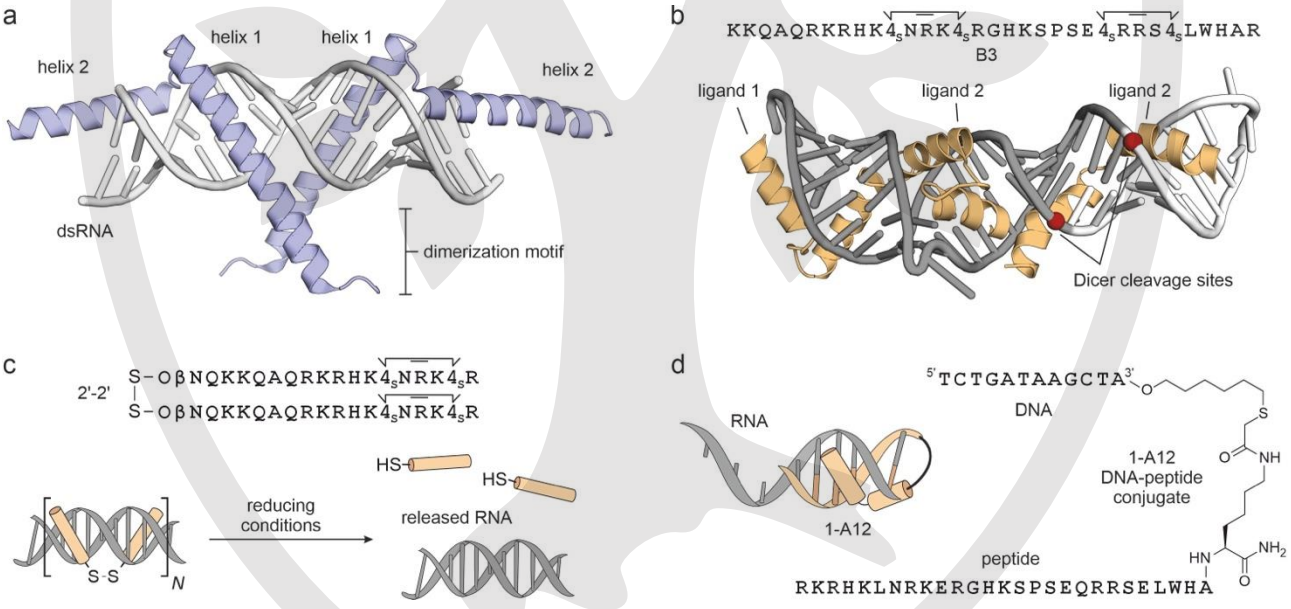

Figure 5| RNA-targeting mimetics: (a) Crystal structure of TAV2b (blue, cartoon representation, PDB ID: 2zi0) bound to palindromic dsRNA (gray).[34] Both helices (1 and 2) and the dimerization motif are indicated. (b) SimRNP model of a complex containing pre-miR-21 (black/gray, cartoon representsation) and three 33-mer peptide ligands (orange). Red spheres indicate the dicer cleavage sites. (c) Cartoon of the homo-dimer derived from helix 1 in TAV2b including the sequence of **2'-2'** (O = 3-mercaptopropanoic acid, β = β-alanine). The homodimer binds double-stranded RNA. Monomerization under reducing conditions leads to RNA release. (d) TAV2b-derived peptide-DNA conjugate **1-A12** which binds single-stranded RNA. The chemical structure of the linker is shown.

The above described TAV2b-derived mimetics do not exhibit pronounced RNA sequence specificity. To facilitate sequence-specific binding of RNA, we designed peptide-DNA hybrids using a truncated version of **wt33** and 10- to 12-mer DNA sequences that were complementary to a single-stranded RNA target (Figure 5d).[37] Notably, we observed 100-fold increased binding affinity to miR-21 when comparing the DNA-peptide conjugate **1-A12** (K_d = 4 nM) with the non-conjugated system (apparent K_d ca. 0.4 µM). For these hybrids, we confirmed sequence-specific binding allowing the execution of selective RNA-templated ligations using a strain-promoted click reaction.[37] Compared to the untemplated reaction, a rate acceleration in the range of two orders of magnitude was achieved.

3 Peptide-based Covalent Protein Modifiers

The use of biocompatible reactions for the covalent modification of proteins is often limited by selectivity issues due to the presence of multiple potential target residues on the protein surface. To address this limitation, we employed proximity-induced reactions[38] that allowed the targeting of certain surface-exposed residues.[8a,39] Our first example of a peptide-directed protein modification used the KIX domain of the CREB binding protein (CBP)[40] as a template for a ligation reaction between two native peptide ligands that bind the KIX domain simultaneously.[39b] One ligand harbored a cysteine while the other presented an appropriately aligned electrophile. Using maleimide as an electrophile, KIX facilitated a templated ligation reaction with a rate acceleration of more than 6000-fold. In this setup, the ligation product exhibited high affinity for the template, preventing reaction turnover and thereby catalytic activity. Using the same trimeric complex but employing a transfer reaction, it was then indeed possible to achieve catalytic turnover (maximum turnover number = 16).[39a]

We also used peptide ligands for the covalent modification and modulation of target proteins. Initial studies used the KIX domain and a KIX-binding motif of mixed-lineage leukemia (MLL). Aiming at the covalent attachment of different labels to the KIX domain, the MLL peptide was equipped with a cysteine-reactive group (chloroacetamide) and a tag (Figure 6a). To study the structural requirements for proximity-induced protein modification, KIX variants with differently positioned cysteines were generated that exhibit varying distances to the electrophile-bearing N-terminus of the peptide (Figure 6b).[39e] As an additional parameter different polyethylene glycol (PEG) spacers were installed between the electrophile and the peptide N-terminus. Subsequently, the reaction rates of all combinations of KIX variants and modified peptides were assessed. The best performing combination (KIX C638 and peptide with PEG_2 linker) was then tested in cell-based experiments using a peptide equipped with a membrane anchor (cationic peptide with fatty acid modification). Microinjection of this probe (**Cl-9L-MA**) into HeLa cells expressing a fluorescently-tagged KIX C638 domain resulted in translocation of this target protein to intracellular membranes. This was the first example of an intracellularly conjugated localization signal and it highlights the potential and selectivity of proximity-induced reactions.

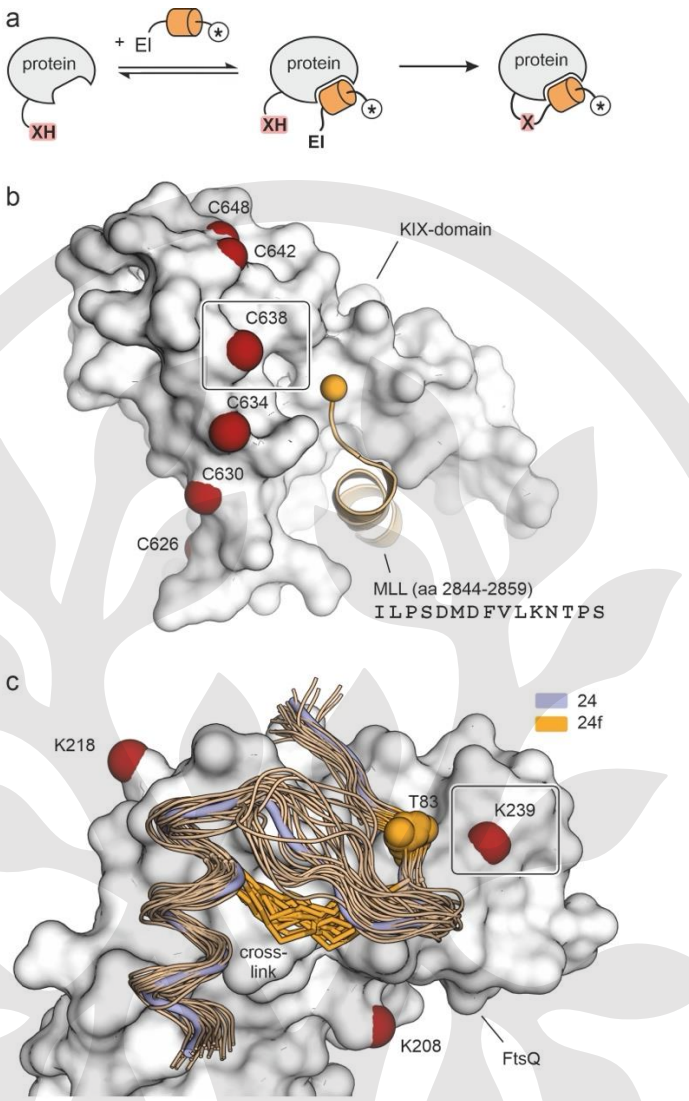

Figure 6| Peptide-based modifiers of proteins. (a) Schematic overview of proximity-induced protein modification reactions. (b) NMR structure (PDB ID: 2lxs) of the KIX-domain of CBP (**P**, white, cartoon representation), with peptide ligand L derived from MLL (orange, cartoon representation, sphere = N-terminus).[40b] Cysteine substitutions (red) were individually introduced. (c) Overlay of crystal structure of peptide **24** (blue, PDB ID 6h90) bound to FtsQ (white, surface representation) and MD-derived binding poses of proteomimetic **24f** (orange, crosslinks are in stick representation).[41] FtsQ lysine residues (red) near the binding site and crosslink in **24f** are highlighted.[8a]

In collaboration with the group of Joen Luirink, we designed electrophile-modified peptides with a covalent mode of action to inhibit interactions between bacterial membrane proteins. Such peptide-based covalent inhibitors have recently gained increasing attention, in particular, when pursuing challenging target proteins.[42] To interfere with the interaction between the bacterial transmembrane proteins FtsQ and FtsB which are both part of the divisome complex, we designed peptidomimetic ligands that target the periplasmic domain of FtsQ using an epitope of FtsB (peptide **24**, blue, Figure 6c) as the starting point.[41] First, the small tertiary structure adopted in the FtsQ-bound state of peptide **24** was stabilized via a hydrocarbon crosslink replicating a salt bridge between the α-helix and a neighboring loop. The resulting proteomimetic **24f** shows good affinity for FtsQ (K_d = 0.45 μM) yet neglectable antibiotic activity even in bacterial strains with leaky

outer membrane to promote periplasmic uptake. To further support target engagement and periplasmic uptake, the peptide was truncated and equipped with a covalent warhead targeting FtsQ lysine K293 in proximity (green, Figure 6c).[8a] After extensive optimization efforts, we obtained 17-mer covalent inhibitor **17fα** which showed activity on clinical isolates of *Escherichia coli* strain when combined with a potentiating stapled peptide.[8a,43]

4 Chemical Protein Engineering

Stabilization of Protein Tertiary Structure

Many biotechnological applications require protein engineering to increase the stability of utilized proteins. Classic strategies invovle protein sequence optimization via consensus-based mutagenesis, directed evolution, or computational approaches.[44] As an alternative, protein macrocyclization approaches have evolved as an appealing strategy to increase the stability of proteins towards thermal and chemical stress.[45] Inspired by bicyclic peptides,[46] we developed the *in situ* cyclization of proteins (INCYPRO) which uses triselectrophilic agents to crosslink three spatially aligned cysteine residues within a protein (Figure 7a).[9] The protein cysteine variants are deigned in a computational, structure-based process aiming for an arrangement of cysteine side-chains that facilitate efficient crosslinking and structure stabilization. Using the KIX domain as a model system, a variety of crosslinkers were investigated (Figure 7b), revealing a direct correlation between crosslink hydrophobicity and stabilizing effect. While all crosslinked KIX versions showed increased thermal stability, the most hydrophilic crosslink (**Ae2**) exhibited the highest stabilizing effect (ΔT_m = 29°C) and the most hydrophobic (**Bz1**) stabilized KIX the least (ΔT_m = 19°C). Crosslink flexibility did not appear to influence protein stability.

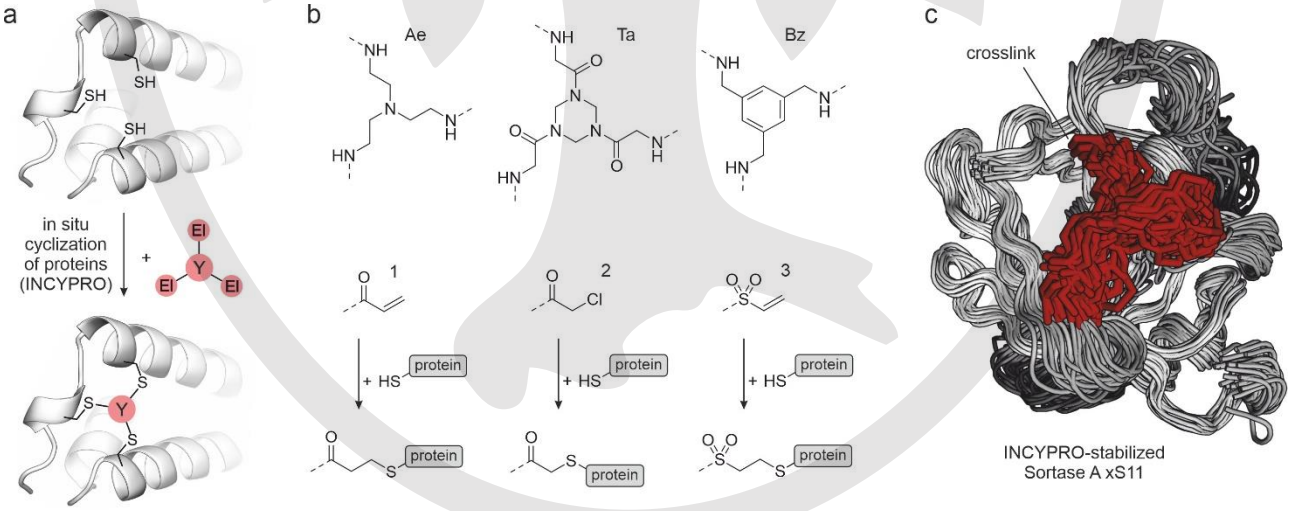

Figure 7| (a) In situ cyclization of proteins (INCYPRO) utilizes three spatially aligned and solvent-exposed cysteines which are reacted with a crosslinker composed of a C3-symmetric core structure (Z) bearing three electrophilic groups (El).[9] (b) Examples of C3-symmetric core structures (Y, top) and electrophilic groups (El, bottom).[47] (c) Molecular dynamics (MD) simulation-derived Structures of INCYPRO-crosslinked Sortase **xS11** (gray: protein, red: crosslink).[48]

Transpeptidase Sortase A (SrtA) and its activity-enhanced version 8M were also stabilized using INCYPRO (Figure 7c).[9,48] Both INCYPRO-stabilized variants (**S7-t1** and **xS11**) showed considerably higher thermal stability than their parent enzymes (ΔT_m = 11 and 12°C, respectively). Importantly, each INCYPRO variant showed enzymatic activity comparable to their parents SrtA and 8M, respectively. Under elevated temperature and in the presence of chemical denaturants such as guanidine hydrochloride (GuHCl) the crosslinked versions, however, exhibited considerably higher activity than their linear counter parts.[48] For example, this allowed the labeling of modified α-synuclein under the denaturing conditions (1 M GuHCl) required for solubilizing its aggregated form.[9]

Stabilization of Quaternary Structure

The stabilization of native protein complexes (quaternary structures) is particularly challenging due to the complexity of involved inter- and intramolecular interactions. As a first example of an INCYPRO-based stabilization of a protein complex, we chose *Pseudomonas fluorescence* esterase (PFE). PFE forms a homo-timeric complex and the introduction of a single cysteine results in three cysteines per protein complex. We introduced one cysteine (per monomer) on each phase of the protein trimer both individually (variants **p2** and **p3**) and in combination (**p4**). In all cases, we obtained efficient crosslinking when using an iodoacetamide-based triselectrophile. Notably, for the trimer of **p4** this resulted in the conjugation of six sites, in three different protein monomers by two crosslinkers (Figure 8a). For the resulting covalently locked trimer **p4$_3$Ta$_2$**, a crystal structure was obtained verifying the expected overall structure and crosslinking sites (Figure 8b).[49] Among the three INCYPRO-stabilized variants, this bicyclic version of PFE showed the highest increase in thermal stability (ΔT_m = 8°C). Most importantly, **p4$_3$Ta$_2$** exhibited a reduced tendency towards aggregation and considerably increased activity under chemical stress. For example, at 1.5 M GuHCl, wt PFF was almost inactive whereas **p4$_3$Ta$_2$** still performed at 15 % of its initial activity. Importantly, crosslinking also conveyed extreme longevity with **p4$_3$Ta$_2$** exhibiting full activity after more than three weeks of storage in PBS at 50°C, while wt PFE showed <10 % activity after 5 days. Subsequently, INCYPRO was applied to four additional homo-trimeric complexes (Figure 8c), all of which exhibited increased thermal stability (ΔT_m = 6 – 39°C).[49]

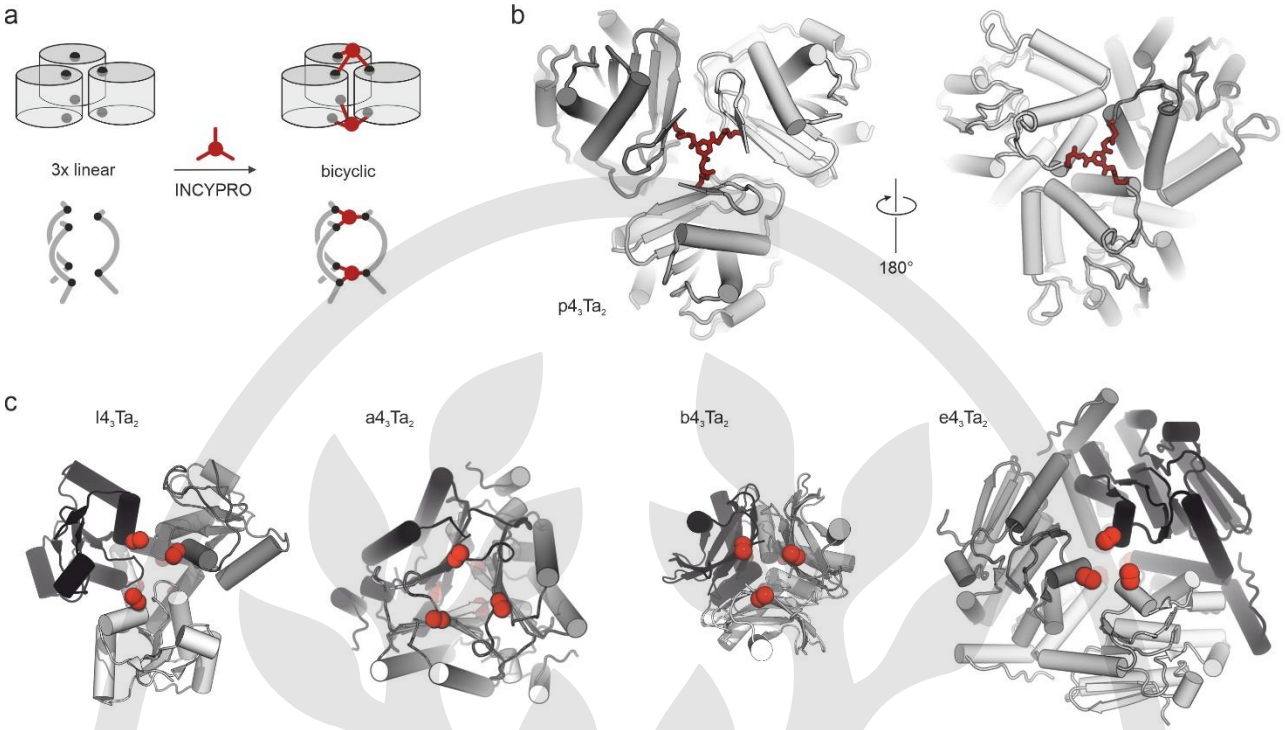

Figure 8| Stabilization of Quaternary Structures: (a) Concept of protein complex bicyclization using INCYPRO. (b) Crystal structure (PDB ID 8pi1) of homotrimeric PFE, **p4$_3$Ta$_2$** (grey, PDB ID 1va4, stick representation) with **Ta4** (red).[49-50] (c) Examples of homotrimeric proteins stabilized with INCYPRO. Crystal structures of timeric parent complexes are shown indicating the crosslinking sites (**l4$_3$Ta$_2$** PDB ID 3fnj; **a4$_3$Ta$_2$**, PDB ID 3c6v; **b4$_3$Ta$_2$** PDB ID 1vmf; **e4$_3$Ta$_2$** PDB ID 5c9g).[49]

5 Conclusions

The adoption of a defined three-dimensional structure is a central aspect of peptide and protein function. Macrocyclization represents an appealing approach to restrict the conformational freedom of these oligomers and thereby stabilize certain three-dimensional structures.[9,45] The variation of macrocyclization scaffolds also provides a means of fine-tuning the degree of flexibility, which is an important aspect of the design process. Chemical crosslinking strategies have given rise to novel peptidomimetic and proteomimetic molecules with enhanced binding characteristics as well as increased resistance to thermal and chemical stress. Constraining the structure of peptide-based scaffolds led to high-affinity binders, resistance to proteolytic degradation, and increased cellular uptake. Although affinity maturation of peptidomimetic structures is a well-established concept, some targets require the stabilization of larger structural motifs and/or the use of a covalent mode-of-action to achieve meaningful inhibitory activities.[42] Notably, the improvement of cellular uptake via conformational constraints is less understood and often requires extensive optimization efforts to achieve sufficient uptake. Overall, peptidomimetics have been used to modulate many levels of biological regulation, targeting proteins as well as nucleic acids.[51] We have also utilized the concept of macrocyclization beyond secondary structures to stabilize entire protein tertiary and quaternary structures. Using a semi-synthetic approach, we have established the *in situ* cyclization of proteins (INCYPRO), a chemical protein engineering approach that alters protein topology, thereby reducing

the tendency of a protein to unfold and aggregate. Taken together, we have developed a broad range of macrocyclization strategies to stabilize the structure of protein-derived molecules ranging from short macrocyclic peptides (*MW* < 1000 g/mol) to large protein complexes (*MW* > 100.000 g/mol). The various approaches discussed in this account highlight the potential of the structure-based design of peptidomimetics and proteomimetics, and how such molecules can contribute to tackle central challenges in diverse fields such as chemical biology, biotechnology and drug discovery.

Biographical Sketches

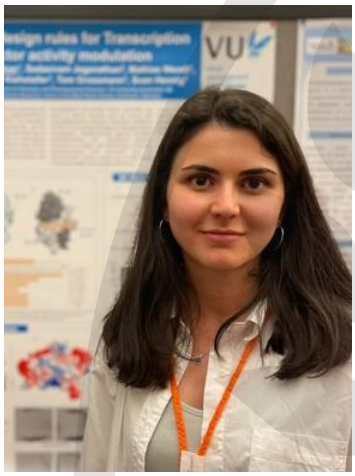

Canan Durukan pursued her undergraduate studies in Chemistry at Yildiz Technical University, and later completed a master's degree in Chemistry at Istanbul Technical University. Since 2020, she has been a PhD candidate in the Grossmann lab, where her research is centered around the inhibition of protein-protein interactions using peptidomimetics.

Tom N. Grossmann is a chemistry professor at the Vrije Universiteit Amsterdam since 2016. He obtained his PhD with Oliver Seitz at the Humboldt-Universität zu Berlin in 2008, and, thereafter, joined Gregory L. Verdine's lab at the Harvard University for postdoctoral research. Tom started as a group leader at the Chemical Genomics Centre and the Technical University in Dortmund before his group moved to Amsterdam. Tom is cofounder of Incircular B.V a university spin-off applying the INCYPRO protein engineering technology.

Acknowledgements

We thank the many group members and collaboration partners that contributed to this work. Particular thanks go to Sven Hennig who was essential to the structural characterization of many of the above mentioned biomimetics. We are gratefull for support by the Fonds der Chemischen Industrie (661413), the German Research Foundation (DFG, Emmy Noether program GR3592/2-1), the European Research Council (ERC starting grant 678623; ERC proof-of-concept 839088, 101067731, 101112973), the Dutch Research Council (NWO 00838037, 01291832), and the Dutch Cancer Society (KWF 15036). This work was also supported by AstraZeneca, Bayer Crop Science, Bayer HealthCare, Boehringer Ingelheim, Merck KGaA, and the Max Planck Society.

Conflict of Interest

T.N.G. is listed as inventors on patent applications related to the INCYPRO stabilization approach as well as β-catenin and RNA-binding peptides. T.N.G. is a co-founder of Incircular B.V. commercializing the INCYPRO technology.

References

(1) (a) J. A. Marsh, S. A. Teichmann, *PLoS biology* **2014**, *12*, e1001870; (b) C. M. Dobson, A. Šali, M. Karplus, *Angewandte Chemie International Edition* **1998**, *37*, 868-893.

(2) (a) S. H. Gellman, *Accounts of chemical research* **1998**, *31*, 173-180; (b) W. S. Horne, T. N. Grossmann, *Nature chemistry* **2020**, *12*, 331-337.

(3) (a) L.-G. Milroy, T. N. Grossmann, S. Hennig, L. Brunsveld, C. Ottmann, *Chemical reviews* **2014**, *114*, 4695-4748; (b) M. Pelay-Gimeno, A. Glas, O. Koch, T. N. Grossmann, *Angewandte Chemie International Edition* **2015**, *54*, 8896-8927; (c) E. Valeur, S. M. Guéret, H. Adihou, R. Gopalakrishnan, M. Lemurell, H. Waldmann, T. N. Grossmann, A. T. Plowright, *Angewandte Chemie International Edition* **2017**, *56*, 10294-10323.

(4) E. Lenci, A. Trabocchi, *Chemical Society Reviews* **2020**, *49*, 3262-3277.

(5) S. Algar, M. Martín-Martínez, R. González-Muñiz, *European Journal of Medicinal Chemistry* **2021**, *211*, 113015.

(6) T. Maculins, J. Garcia-Pardo, A. Skenderovic, J. Gebel, M. Putyrski, A. Vorobyov, P. Busse, G. Varga, M. Kuzikov, A. Zaliani, *Cell Chemical Biology* **2020**, *27*, 1441-1451. e1447.

(7) (a) A. Glas, D. Bier, G. Hahne, C. Rademacher, C. Ottmann, T. N. Grossmann, *Angewandte Chemie International Edition* **2014**, *53*, 2489-2493; (b) M. Wendt, R. Bellavita, A. Gerber, N. L. Efrém, T. van Ramshorst, N. M. Pearce, P. R. Davey, I. Everard, M. Vazquez-Chantada, E. Chiarparin, *Angewandte Chemie International Edition* **2021**, *60*, 13937-13944.

(8) (a) F. M. Paulussen, G. K. Schouten, C. Moertl, J. Verheul, I. Hoekstra, G. M. Koningstein, G. H. Hutchins, A. Alkir, R. A. Luirink, D. P. Geerke, *Journal of the American Chemical Society* **2022**, *144*, 15303-15313; (b) H. Adihou, R. Gopalakrishnan, T. Förster, S. M. Guéret, R. Gasper, S. Geschwindner, C. Carrillo García, H. Karatas, A. V. Pobbati, M. Vazquez-Chantada, *Nature Communications* **2020**, *11*, 5425.

(9) M. Pelay-Gimeno, T. Bange, S. Hennig, T. N. Grossmann, *Angewandte Chemie International Edition* **2018**, *57*, 11164-11170.

(10) G. H. Hutchins, S. Kiehstaller, P. Poc, A. H. Lewis, J. Oh, R. Sadighi, N. M. Pearce, M. Ibrahim, I. Drienovská, A. M. Rijs, *Chem* **2023**, *10*, 615-627.

(11) (a) P. M. Cromm, J. Spiegel, T. N. Grossmann, *ACS chemical biology* **2015**, *10*, 1362-1375; (b) Q. Chu, R. E. Moellering, G. J. Hilinski, Y.-W. Kim, T. N. Grossmann, J. T.-H. Yeh, G. L. Verdine, *MedChemComm* **2015**, *6*, 111-119; (c) Y.-W. Kim, T. N. Grossmann, G. L. Verdine, *Nature protocols* **2011**, *6*, 761-771; (d) C. E. Schafmeister, J. Po, G. L. Verdine, *Journal of the American Chemical Society* **2000**, *122*, 5891-5892.

(12) A. Glas, T. N. Grossmann, *Synlett* **2015**, *26*, 1-5.

(13) A. Glas, E. C. Wamhoff, D. M. Krüger, C. Rademacher, T. N. Grossmann, *Chemistry–A European Journal* **2017**, *23*, 16157-16161.

(14) D. M. Krüger, A. Glas, D. Bier, N. Pospiech, K. Wallraven, L. Dietrich, C. Ottmann, O. Koch, S. Hennig, T. N. Grossmann, *Journal of medicinal chemistry* **2017**, *60*, 8982-8988.

(15) K. Wallraven, F. L. Holmelin, A. Glas, S. Hennig, A. I. Frolov, T. N. Grossmann, *Chemical science* **2020**, *11*, 2269-2276.

(16) P. M. Cromm, K. Wallraven, A. Glas, D. Bier, A. Fürstner, C. Ottmann, T. N. Grossmann, *ChemBioChem* **2016**, *17*, 1915-1919.

(17) H. E. Blackwell, R. H. Grubbs, *Angewandte Chemie International Edition* **1998**, *37*, 3281-3284.

(18) C. Toniolo, M. Crisma, F. Formaggio, C. Valle, G. Cavicchioni, G. Precigoux, A. Aubry, J. Kamphuis, *Biopolymers: Original Research on Biomolecules* **1993**, *33*, 1061-1072.

(19) (a) P. M. Cromm, J. Spiegel, T. N. Grossmann, H. Waldmann, *Angewandte Chemie International Edition* **2015**, *54*, 13516-13537; (b) J. Spiegel, P. M. Cromm, G. Zimmermann, T. N. Grossmann, H. Waldmann, *Nature chemical biology* **2014**, *10*, 613-622.

(20) J. Spiegel, P. M. Cromm, A. Itzen, R. S. Goody, T. N. Grossmann, H. Waldmann, *Angewandte Chemie International Edition* **2014**, *53*, 2498-2503.

(21) P. M. Cromm, J. Spiegel, P. Küchler, L. Dietrich, J. Kriegesmann, M. Wendt, R. S. Goody, H. Waldmann, T. N. Grossmann, *ACS chemical biology* **2016**, *11*, 2375-2382.

(22) P. M. Cromm, S. Schaubach, J. Spiegel, A. Fürstner, T. N. Grossmann, H. Waldmann, *Nature communications* **2016**, *7*, 11300.

(23) S. Jeganathan, M. Wendt, S. Kiehstaller, D. Brancaccio, A. Kuepper, N. Pospiech, A. Carotenuto, E. Novellino, S. Hennig, T. N. Grossmann, *Angewandte Chemie* **2019**, *131*, 17512-17519.

(24) M. Nardini, N. Gnesutta, G. Donati, R. Gatta, C. Forni, A. Fossati, C. Vonrhein, D. Moras, C. Romier, M. Bolognesi, *Cell* **2013**, *152*, 132-143.

(25) C. Durukan, F. Arbore, R. Klintrot, C. Bigiotti, I. M. Ilie, J. Vreede, T. N. Grossmann, S. Hennig, *ChemBioChem* **2024**, e202400020.

(26) S. Jiao, H. Wang, Z. Shi, A. Dong, W. Zhang, X. Song, F. He, Y. Wang, Z. Zhang, W. Wang, *Cancer cell* **2014**, *25*, 166-180.

(27) (a) E. M. Koelman, A. Yeste-Vázquez, T. N. Grossmann, *Bioorganic & Medicinal Chemistry* **2022**, *70*, 116920; (b) G. Hahne, T. N. Grossmann, *Bioorganic & medicinal chemistry* **2013**, *21*, 4020-4026.

(28) M. A. McCoy, D. Spicer, N. Wells, K. Hoogewijs, M. Fiedler, M. G. Baud, *Journal of Medicinal Chemistry* **2022**, *65*, 7246-7261.

(29) T. N. Grossmann, J. T.-H. Yeh, B. R. Bowman, Q. Chu, R. E. Moellering, G. L. Verdine, *Proceedings of the National Academy of Sciences* **2012**, *109*, 17942-17947.

(30) A. Held, A. Glas, L. Dietrich, M. Bollmann, K. Brandstädter, T. Grossmann, C. Lohmann, T. Pap, J. Bertrand, *Osteoarthritis and Cartilage* **2018**, *26*, 818-823.

(31) L. Dietrich, B. Rathmer, K. Ewan, T. Bange, S. Heinrichs, T. C. Dale, D. Schade, T. N. Grossmann, *Cell chemical biology* **2017**, *24*, 958-968. e955.

(32) A. H. Huber, W. I. Weis, *Cell* **2001**, *105*, 391-402.

(33) (a) B. Ellenbroek, J. P. Kahler, S. R. Evers, S. J. Pomplun, *Angewandte Chemie International Edition* **2024**, e202401704; (b) S. Pal, P. 't Hart, *Frontiers in Molecular Biosciences* **2022**, *9*, 883060.

(34) H. Y. Chen, J. Yang, C. Lin, Y. A. Yuan, *EMBO reports* **2008**, *9*, 754-760.

(35) A. Kuepper, N. M. McLoughlin, S. Neubacher, A. Yeste-Vázquez, E. Collado Camps, C. Nithin, S. Mukherjee, L. Bethge, J. M. Bujnicki, R. Brock, *Nucleic acids research* **2021**, *49*, 12622-12633.

(36) N. M. McLoughlin, M. A. Albers, E. Collado Camps, J. Paulus, Y. A. Ran, S. Neubacher, S. Hennig, R. Brock, T. N. Grossmann, *Angewandte Chemie* **2023**, e202308028.

(37) N. M. McLoughlin, A. Kuepper, S. Neubacher, T. N. Grossmann, *Chemistry–A European Journal* **2021**, *27*, 10477-10483.

(38) K. Shiraiwa, R. Cheng, H. Nonaka, T. Tamura, I. Hamachi, *Cell Chemical Biology* **2020**, *27*, 970-985.

(39) (a) N. Brauckhoff, L. Fang, A. Haim, T. N. Grossmann, *Chemical Communications* **2023**, *59*, 5241-5244; (b) N. Brauckhoff, G. Hahne, J. T. H. Yeh, T. N. Grossmann, *Angewandte Chemie International Edition* **2014**, *53*, 4337-4340; (c) C. U. Lee, T. N. Grossmann, *Angewandte Chemie International Edition* **2012**, *35*, 8699-8700; (d) C. U. Lee, G. Hahne, J. Hanske, T. Bange, D. Bier, C. Rademacher, S. Hennig, T. N. Grossmann, *Angewandte Chemie International Edition* **2015**, *54*, 13796-13800; (e) C. Stiller, D. M. Krüger, N. Brauckhoff, M. Schmidt, P. Janning, H. Salamon, T. N. Grossmann, *ACS chemical biology* **2017**, *12*, 504-509.

(40) (a) C. Mueller, T. N. Grossmann, *Angew Chem Int Ed Engl* **2018**, *57*, 17079-17083; (b) S. Brüschweiler, R. Konrat, M. Tollinger, *ACS chemical biology* **2013**, *8*, 1600-1610.

(41) D. Kureisaite-Ciziene, A. Varadajan, S. H. McLaughlin, M. Glas, A. Montón Silva, R. Luirink, C. Mueller, T. Den Blaauwen, T. N. Grossmann, J. Luirink, *MBio* **2018**, *9*, 10.1128/mbio. 01346-01318.

(42) F. M. Paulussen, T. N. Grossmann, *Journal of Peptide Science* **2023**, *29*, e3457.

(43) G. K. Schouten, F. M. Paulussen, O. P. Kuipers, W. Bitter, T. N. Grossmann, P. van Ulsen, *Antibiotics* **2022**, *11*, 273.

(44) (a) T. J. Magliery, *Current opinion in structural biology* **2015**, *33*, 161-168; (b) A. M. Chapman, B. R. McNaughton, *Cell chemical biology* **2016**, *23*, 543-553; (c) M. T. Reetz, *Angewandte Chemie International Edition* **2013**, *10*, 2658-2666.

(45) A. Haim, S. Neubacher, T. N. Grossmann, *ChemBioChem* **2021**, *22*, 2672-2679.

(46) (a) B. Dang, H. Wu, V. K. Mulligan, M. Mravic, Y. Wu, T. Lemmin, A. Ford, D.-A. Silva, D. Baker, W. F. DeGrado, *Proceedings of the National Academy of Sciences* **2017**, *114*, 10852-10857; (b) S. Chen, D. Bertoldo, A. Angelini, F. Pojer, C. Heinis, *Angewandte Chemie International Edition* **2014**, *53*, 1602-1606; (c) C. Heinis, T. Rutherford, S. Freund, G. Winter, *Nature chemical biology* **2009**, *5*, 502-507; (d) P. Timmerman, J. Beld, W. C. Puijk, R. H. Meloen, *ChemBioChem* **2005**, *6*, 821-824.

(47) S. Neubacher, J. M. Saya, A. Amore, T. N. Grossmann, *The Journal of Organic Chemistry* **2019**, *85*, 1476-1483.

(48) S. Kiehstaller, G. H. Hutchins, A. Amore, A. Gerber, M. Ibrahim, S. Hennig, S. Neubacher, T. N. Grossmann, *Bioconjugate chemistry* **2023**, *34(6)*, 1114-1121.

(49) G. H. Hutchins, S. Kiehstaller, P. Poc, A. H. Lewis, J. Oh, R. Sadighi, N. M. Pearce, M. Ibrahim, I. Drienovská, A. M. Rijs, *Chem* **2024**, *10*, 615-627.

(50) J. D. Cheeseman, A. Tocilj, S. Park, J. D. Schrag, R. J. Kazlauskas, *Acta Crystallographica Section D: Biological Crystallography* **2004**, *60*, 1237-1243.

(51) N. M. McLoughlin, C. Mueller, T. N. Grossmann, *Cell chemical biology* **2018**, *25*, 19-29.